Multidrug resistance-associated protein 3 and Bcl-2 contribute to multidrug resistance by vinorelbine in lung adenocarcinoma

XUAN HONG[1], ZHAO-YANG YANG[1], MENG WANG[1], LU LU[2], YING-HONG LI[1], XISHAN HAO[3] and GONG-YAN CHEN[1]

[1]Department of Medical Oncology, The Third Affiliated Hospital of Harbin Medical University; [2]Department of Medical Oncology, The Fourth Affiliated Hospital of Harbin Medical University; [3]Department of General Surgery, The Tumor Hospital of Tianjin Medical University, P.R. China

Received May 23, 2011; Accepted July 4, 2011

DOI: 10.3892/ijmm.2011.779

Abstract. Although cancer cells initially respond to vinorelbine (NVB), the acquisition of resistance to the treatment is the main cause of chemotherapeutic failure in lung cancer. The intrinsic mechanism of drug resistance induced by NVB in lung cancer is not clear and tumor cell models to study NVB resistance have not been widely studied. We previously established a NVB resistant cell line, Anip973/NVB, derived from the Anip973 lung adenocarcinoma cell line. The aim of this study was to investigate the molecular mechanisms involved in the resistance to NVB in lung adenocarcinoma. Genetic profiles of Anip973/NVB and Anip973 cells were compared by microarray analysis and qRT-PCR. Tumor xenografts were obtained by grafting Anip973/NVB and Anip973 cells into nude mice and the xenograft response to NVB or control treatment was evaluated. Morphological assessment of xenograft tissues was performed by transmission electron microscopy (TEM). Immunohistochemistry (IHC) was used to compare Bcl-2 and MRP3 protein expression in xenografts. Fifty-five up-regulated genes and 88 down-regulated genes in Anip973/NVB cells compared with Anip973 cells were identified by cDNA microarray analysis. Up-regulation of MRP3 and Bcl-2 was confirmed by qRT-PCR. NVB inhibits xenografts of Anip973 growth but did not affect xenografts of Anip973/NVB growth. Ultrastructural changes observed by TEM showed that NVB induces apoptosis in the Anip973-treated group but not in the Anip973/NVB-treated group. Higher expression rates of Bcl-2 and MRP3 were observed in Anip973/NVB xenograft cells compared with Anip973 xenograft cells by IHC. In conclusion, in the present study, we identified a set of genes responsible for multidrug resistance in Anip973/NVB cells. Among them, MRP3 and Bcl-2 may participate in lung adenocarcinoma multidrug resistance induced by NVB.

Correspondence to: Dr Gong-Yan Chen, Department of Medical Oncology, The Third Affiliated Hospital of Harbin Medical University, Haping Road 150, Harbin 150081, P.R. China
E-mail: chengongyan@medmail.com.cn

Key words: vinorelbine, multidrug resistance, lung adenocarcinoma, MRP3, Bcl-2

Introduction

Vinorelbine (Navelbine, NVB, 3,4'-didehydro-4'deoxy-*C*'-vinorelbine) is used for chemotherapy of malignancy since the 1990s, and it is chemically different from vinblastine by substitutions on the catharantine moiety of the molecule and is found to bind to the membrane vesicles more intensively than vincristine (1,2). NVB is one of first-line chemotherapeutic drugs for non-small cell lung cancer (NSCLC) patients. The effective rates of the anticancer agent for NSCLC were reported to be between 14-33% and up to about 50% in combination chemotherapy with cisplatin, and it is regarded as one of the most effective drugs for NSCLC (3-5). However, although the tumors initially respond to NVB, the acquisition of NVB resistance used in chemotherapy is still the main cause of treatment failure in malignancy. Similarly with cisplatin, resistance of lung cancer cells to NVB is usually accompanied by resistance to other drugs with different structures and cellular targets (6,7). Very little is known about the intrinsic mechanism for inducing multidrug resistance by NVB until now. Identifying the molecular detail leading to acquired multidrug resistance to NVB may be important in developing more effective therapies.

The intrinsic mechanism of drug resistance induced by NVB is not clear and tumor cell models to study NVB resistance are rare until now. We thus established an NVB-resistant cell line from the lung adenocarcinoma Anip973 cell line and named it Anip973/NVB in a previous study (8). The sensitivities of Anip973/NVB cells to various chemotherapeutics were determined by MTT assay. Our previous study showed that the resistance index of the Anip973/NVB cells to NVB was 21.81, and Anip973/NVB cells had multidrug resistant characteristic to several drugs, such as cisplatin, paclitaxel, etoposide, isofosfamide, fluorouracil, dacarbazine, pharmorubicin, with resistance indices of 11.89, 11.68, 6.12, 3.95, 2.86, 2.64 and 2.15, respectively. Nevertheless, the cells still remained sensitive to irinotecan and gemcitabine.

In order to study the mechanism on multidrug resistance by NVB in lung adenocarcinoma, we investigated the gene expression variance between the Anip973/NVB and Anip973

cell lines by DNA microarray and qRT-PCR. Then xenografts of Anip973/NVB and Anip973 cells were established to investigate selected drug-resistance proteins.

Materials and methods

Cell lines. The human lung adenocarcinoma cell line, Anip973, was kindly provided by the Tumor Research Institute of Harbin Medical University. The Anip973/NVB cell line was established by slowly increasing the concentration of NVB (Laboratories Pierre Fabre, France) and its biological characteristics were confirmed (8). Anip973 and Anip973/NVB cells were cultured in RPMI-1640 (HyClone, USA) medium supplemented with 10% fetal bovine serum, penicillin (100 U/ml) and streptomycin (100 μg/ml) (Invitrogen, Gaithersburg, MD, USA) in standard culture condition (95% air, 5% CO_2, 37˚C).

Microarray assays and analysis. Human gene oligonucleotide arrays (CapitalBio, China) which contained 7-mer length DNA from 21571 genes was used. Total-RNA was isolated from Anip973 and Anip973/NVB cells using the TRIzol reagent (Invitrogen) according to manufacturer's instructions. Integrity of the RNA was determined by spectrophotometry and electrophoresis. Total-RNA was reverse transcribed into cDNA by the cDNA synthesis kit (Promega, USA). Cy3-dUTP or Cy5-dUTP (Amersham Pharmacia Biotech, USA) was incorporated during reverse transcription of 10 μg of total-RNA and primed by T_7-Oligo(dt)15 primer (Boya, China). Different fluorescent-labeled probes from Anip973 and Anip973/NVB were mixed. After incubation at 42˚C overnight in a humidified environment, fluorescent images of hybridized microarrays were scanned with LuxScan 10KA dual channel laser scanner (CapitalBio) using GenePix Pro 4.0 image analysis software (Axon Instruments, USA) according to the manufacturer's instructions. To control labeling differences, the experiment was carried out three times, in which the fluorescent dyes were switched during cDNA synthesis for each cell line. The two ratios were then multiplied to generate the ratio of Anip973/NVB to Anip973 cells, and one gene was considered to be significantly differentially expressed if its ratio was >2 in all three experiments.

Quantitative reverse transcription-PCR. Total-RNA was isolated from Anip973 and Anip973/NVB cells using the TRIzol reagent (Invitrogen). cDNA was synthesized from isolated RNA using the RevertAid™ First Strand cDNA Synthesis kit (MBI, USA) according to manufacturer's instructions. The expression levels of MRP1, MRP3, MDR1, Bcl-2 were validated by real-time quantitative reverse transcription PCR (qRT-PCR). The SYBR-Green master mix from Applied Biosystems was used. qRT-PCR was performed using the ABI PRISM 7000 Sequence Detection system (Applied Biosystems). The C_T value of mRNA expression for each sample were normalized with the internal housekeeping gene β-actin and relative quantitation values were plotted.

The primer sequences of each gene for real-time qPCR were as follows: MDR1, forward, 5'-ATTTCTATAGGTGCT-3' and reverse, 5'-CCGTAGAAACCTTAC-3'; MRP1, forward, 5'-GGACCTGGACTTCGTTCTCA-3' and reverse, 5'-CGTCCAGACTTCTTCATCCG-3'; MRP3, forward, 5'-GCACCATTGTCGTGGCTACA-3' and reverse, 5'-GCAGGACACCCAGGACCAT-3'; Bcl-2, forward, 5'-TGCACCTGACGCCCTTCAC-3' and reverse, 5'-AGACAGCCAGGAGAAATCAAACAG-3'; β-actin, forward, 5'-GCTGGAAGGTGGACAGCGA-3' and reverse, 5'-GGCATCGTGATGGACTCCG-3'.

Establishment of tumor xenografts. All studies were approved by the institutional animal care and use committee, and they were carried out in accordance with institutional guidelines for animal care. The female BALB/C nude mice were provided by the Beijing Animal Research Institute. The animals were 4-6-weeks-old and weighed 17-21 grams on the day of tumor implantation. Each nude mouse was inoculated with 1 ml of $1x10^7$ cells subcutaneously via the left armpit. The 12 models were established with Anip973 cells and the other 12 models were established with the Anip973/NVB cells. When tumors grew to 5-10 mm in diameter, the animals were grouped and then managed.

The 2 xenograft models were equally assigned to 2 treatment groups respectively: 6 mice for Anip973 cells and 6 mice for Anip973/NVB cells were treated with 0.2 ml of 20 mg/kg NVB via the vena caudalis (treated groups) and 6 mice for Anip973 cells and 6 mice for Anip973/NVB cells were treated with 0.2 ml of saline in the same way (untreated groups). After 7 days, the mice were sacrificed and the tumors were excised and tumor volumes were measured. The size of the tumors was determined by measuring length (the longest diameter) and width (the shortest diameter). The tumor volume was calculated using the formula: volume = width^2 x length x 0.52. The tumor growth inhibition rate (IR) was calculated according to the volume of the tumor: IR (%) = (1-volume of treated group/volume of untreated group) x 100%.

Morphological assessment of apoptosis of xenograft tissues. After the mice were sacrificed, the xenograft tissues were excised and cut into small pieces (1x1 mm), fixed with 2.5% glutaraldehyde and phosphate buffer solution for 3 h and washed with 0.1 M sodium phosphate buffer, post-fixed with 1% osmium tetroxide, dehydrated in graded ethanol and acetonum, embedded in Epon 812 mixture and cut into sections with 50 nm thickness using an ultramicrotome (Leica, China). After staining with uranyl acetate and lead citrate, the sections were examined by transmission electron microscopy (TEM) (Hitachi-500, Japan).

Immunohistochemical analysis. Excised tumors were embedded in formalin-fixed paraffin and then sectioned into 4 μm thick sections, and mounted on glass slides. After deparaffinization, the tissue sections were heated at 120˚C for 15 min in 10 mM Tris-HCl with 1 mM EDTA (pH 9.0). Endogenous peroxidase was blocked with 3% hydrogen peroxide in methanol for 10 min at room temperature. The sections were incubated overnight at 4˚C with antibodies against Bcl-2 (Santa Cruz Biotechnology, Santa Cruz, CA, USA) at a 1:200 dilution and MRP3 (Santa Cruz Biotechnology) at a 1:300 dilution. Then biotinylated immunoglobulin and streptavidin conjugated to peroxidase were added. Finally, 3,3'-diaminobenzidine was added for color development, and hematoxylin was used for counterstaining. Negative controls processed without the primary antibody were performed in each experiment. The mean percentage of positive tumor cells was determined in at least five areas at x400

Table I. The 143 genes up-regulated and down-regulated between Anip973 and Anip973/NVB cells by microarray analysis.

Accession no.	Gene name	Gene description	Ratio
NM003726	SCAP1	Src family associated phosphoprotein 1	30.6889
NM033292	CASP1	Caspase 1, apoptosis-related cysteine protease (interleukin 1, β, convertase)	16.2552
NM000700	ANXA1	Annexin A1	13.3031
NM001353	AKRIC1	Aldo-keto reductase family 1, member C1 (dihydrodiol dehydrogenase 1; 20-α (3-α)-hydroxysteroid dehydrogenase)	10.4311
NM001818	AKRIC4	Aldo-keto reductase family 1, member C4 (chlordecone reductase; 3-α hydroxysteroid dehydrogenase)	10.3319
NM020038	MRP3	ATP-binding cassette, sub-family C (CFTR/MRP), member 3	3.9728
NM016234	ACSL5	Fatty-acid-coenzyme A ligase, long-chain 5	3.7045
NM004572	PKP2	Plakophilin 2	3.5271
NM024563	FLJ14054	Hypothetical protein FLJ14054	3.4879
NM003054	SLC18A2	Solute carrier family 18 (vesicular monoamine), member 2	3.2583
NM002015	FOXO1A	Forkhead box O1A (rhabdomyosarcoma)	3.2449
NM001218	CA12	Carbonic anhydrase XII	3.1765
NM000602	SERPINE1	Serine (or cysteine) proteinase inhibitor, clade E (nexin, plasminogen activator inhibitor type 1)	3.1525
NM024659	FLJ11753	Hypothetical protein FLJ11753	3.0686
NM002539	ODC1	Ornithine decarboxylase 1	2.8646
AF072928	MTMR6	Myotubularin-related protein 6	2.8512
AK057568	INE2	Inactivation escape 2	2.8102
AF019226	GOV	Glioblastoma overexpressed	2.7968
BC017984	LOC338769	*Homo sapiens*, clone IMAGE: 4245930, mRNA	2.7906
NM032883	C20orf100	Chromosome 20 open reading frame 100	2.7100
AK055962	ARG99	ARG99 protein	2.6579
NM002097	GTF3A	General transcription factor IIIA	2.6531
NM001855	COL15A1	Collagen, type XV, α 1	2.6529
NM020987	ANK3	Ankyrin 3, node of Ranvier (ankyrin G)	2.6458
AB058718	KIAA1815	Hypothetical protein FLJ23309	2.5897
AF218006	FLJ13612	Hypothetical protein FLJ13612	2.5560
NM024696	FLJ23058	Hypothetical protein FLJ23058	2.5358
NM006437	PARP4	ADP-ribosyltransferase (NAD^+; poly (ADP-ribose) polymerase)-like 1	2.5014
NM002620	PF4V1	Platelet factor 4 variant 1	2.4987
NM003558	PIP5K1B	Unc-13-like (*C. elegans*)	2.4719
NM002317	LOX	Lysyl oxidase	2.4123
BC015417	MGC21981	Homo sapiens, clone MGC: 21981 IMAGE: 4396073, mRNA, complete cds	2.4026
NM002061	GCLM	Glutamate-cysteine ligase, modifier subunit	2.3993
NM003039	SLC2A5	Solute carrier family 2 (facilitated glucose/fructose transporter), member 5	2.3748
NM033128	SCIN	Scinderin	2.3618
NM001038	SCNN1A	Sodium channel, nonvoltage-gated 1 α	2.3547
NM004751	GCNT3	Glucosaminyl (N-acetyl) transferase 3, mucin type	2.3368
SK025736	HMGCS1	3-Hydroxy-3-methylglutaryl-coenzyme a synthase 1 (soluble)	2.3321
NM000716	C4BPB	Complement component 4 binding protein, β	2.3225
NM005857	ZMPSTE24	Zinc metalloproteinase (STE24 homolog, yeast)	2.3135
NM001498	GCLC	Glutamate-cysteine ligase, catalytic subunit	2.3049
NM004105	EFEMP1	EGF-containing fibulin-like extracellular matrix protein 1	2.2991
AB018271	KIAA0728	KIAA0728 protein	2.2949
NM016542	MST4	Serine/threonine protein kinase MASK	2.2656
AL050201	C6orf162	Hypothetical protein DKFZp586E1923	2.2518
BC010117	MGC13038	Hypothetical protein MGC13038	2.2448
NM002395	ME1	Malic enzyme 1, NADP(+)-dependent, cytosolic	2.2398
NM000908	NPR3	Natriuretic peptide receptor C/guanylate cyclase C (atrionatriuretic peptide receptor C)	2.2196
NM000237	LPL	Lipoprotein lipase	2.2196
NM004529	MLLT3	Myeloid/lymphoid or mixed-lineage leukemia (trithorax homolog, *Drosophila*); translocated to, 3	2.2057
AB002351	DMN	Desmuslin	2.1525
D80010	LPIN1	Lipin 1	2.1335
NM022358	KCNK15	Potassium channel, subfamily K, member 15 (TASK-5)	2.1214
NM001845	COL4A1	Collagen, type IV, α 1	2.1074

Table I. Continued.

Accession no.	Gene name	Gene description	Ratio
AK000160	MYO1B	Myosin IB	2.0118
AF361486	MUC16	Mucin 16	0.4869
NM014279	OLFM1	Olfactomedin 1	0.4856
NM004494	HDGF	Hepatoma-derived growth factor (high-mobility group protein 1-like)	0.4652
AF070673	SNN	Stannin	0.4634
AL390079	LOC58489	Hypothetical protein from EUROIMAGE 588495	0.4594
NM001908	CTSB	Cathepsin B	0.4572
NM000480	AMPD3	Adenosine monophosphate deaminase (isoform E)	0.4489
AB011100	KIAA0528	KIAA0528 gene product	0.4419
NM005239	ETS2	V-ets erythroblastosis virus E26 oncogene homolog 2 (avian)	0.4393
AB040879	KIAA1446	KIAA1446 protein	0.4371
AF217965	PTGES	Prostaglandin E synthase	0.4261
NM006622	PLK2	Serum-inducible kinase	0.4178
NM002583	PAWR	PRKC, apoptosis, WT1, regulator	0.4095
NM001902	CTH	Cystathionase (cystathionine γ-lyase)	0.4061
NM031915	SETDB2	CLLL8 protein	0.4053
NM001848	COL6A1	Collagen, type VI, α 1	0.4004
AF022789	USP12	Ubiquitin specific protease 12	0.3945
AJ311123	DKFZP434A1114	Hypothetical gene DKFZp434A1114	0.3939
NM001089	ABCA3	ATP-binding cassette, sub-family A (ABC1), member 3	0.392
NM012168	FBXO2	F-box only protein 2	0.3916
NM024808	FLJ22624	Hypothetical protein FLJ22624	0.3908
NM024110	CARD14	Caspase recruitment domain protein 14	0.3898
NM021012	KCNJ12	Potassium inwardly-rectifying channel, subfamily J, member 12	0.3878
NM000362	TIMP3	Tissue inhibitor of metalloproteinase 3 (sorsby fundus dystrophy, pseudoinflammatory)	0.3869
NM031412	GABARAPL1	GABA(A) receptor-associated protein like 1	0.3865
AK024478	FLJ11305	Hypothetical protein FLJ11305	0.3857
NM014116	MED4	HSPC126 protein	0.3818
NM002414	CD99	Antigen identified by monoclonal antibodies 12E7, F21 and O13	0.3745
NM017720	FLJ20234	Hypothetical protein FLJ20234	0.3723
NM003069	SMARCA1	SWI/SNF related, matrix associated, actin dependent regulator of chromatin, subfamily a, member 1	0.3695
NM017905	C13orf11	Hypothetical protein FLJ20623	0.3693
NM002961	S100A4	S100 calcium binding protein A4 (calcium protein, calvasculin, metastasin, murine placental homolog)	0.3636
AK056841	KCNRG	*Homo sapiens* cDNA FLJ32279 fis, clone PROST2000165	0.3595
NM007150	ZNF185	Zinc finger protein 185 (LIM domain)	0.3579
NM018214	LANO	LAP (leucine-rich repeats and PDZ) and no PDZ protein	0.3552
D83076	KIAA0239	KIAA0239 protein	0.3538
NM006186	NR4A2	Nuclear receptor subfamily 4, group A, member 2	0.3534
NM025206	FER1L4	Fer-1-like 4 (*C. elegans*)	0.3529
NM003652	CPZ	Carboxypeptidase Z	0.3527
AK027071	TSC22	Transforming growth factor β-stimulated protein TSC-22	0.3522
U67784	RDC1	G protein-coupled receptor	0.3517
NM002747	MAPK4	Mitogen-activated protein kinase 4	0.3506
NM032401	TMPRSS3	Transmembrane protease, serine 3	0.3493
NM018584	PRO1489	Hypothetical protein PRO1489	0.3461
NM052811	RFP2	Ret finger protein 2	0.3448
NM001200	BMP2	Bone morphogenetic protein 2	0.3363
NM000213	ITGB4	Integrin, β 4	0.3350
NM014448	ARHGEF16	Rho guanine exchange factor (GEF) 16	0.3322
NM019045	WDR44	Similar to rab11-binding protein	0.3294
NM000683	ADRA2C	Adrenergic, α-2C-, receptor	0.3269
NM004221	NK4	Natural killer cell transcript 4	0.3242
NM012331	MSRA	Methionine sulfoxide reductase A	0.3164
NM003186	TAGLN	Transgelin	0.3045

Table I. Continued.

Accession no.	Gene name	Gene description	Ratio
NM001632	ALPP	Alkaline phosphatase, placental (regan isozyme)	0.2972
NM005245	FAT	FAT tumor suppressor homolog 1 (*Drosophila*)	0.2970
D25304	ARHGEF6	Rac/Cdc42 guanine nucleotide exchange factor (GEF) 6	0.2942
AB021124	CHST2	Carbohydrate (N-acetylglucosamine-6-O) sulfotransferase 2	0.2905
NM001381	DOK1	Docking protein 1, 62kD (downstream of tyrosine kinase 1)	0.2837
NM003820	TNFRSF14	Tumor necrosis factor receptor superfamily, member 14 (herpesvirus entry mediator)	0.2786
NM052947	ALPK2	Heart α-kinase	0.2784
NM018306	FLJ11036	Hypothetical protein FLJ11036	0.2778
AF323540	APOL1	Apolipoprotein L, 1	0.2770
NM016602	CCR10	G protein-coupled receptor 2	0.2754
AF018081	COL18A1	Collagen, type XVIII, α 1	0.2662
NM018478	C20orf35	Chromosome 20 open reading frame 35	0.2579
NM002193	INHBB	Inhibin, β B (activin AB β polypeptide)	0.2430
NM000273	GPR143	Ocular albinism 1 (Nettleship-Falls)	0.2383
AF217974	DKFZP434K1772	Hyothetical protein	0.2307
NM000422	KRT17	Keratin 17	0.2246
AK001520	LOC153218	*Homo sapiens* cDNA FLJ10658 fis, clone NT2RP2006052	0.2089
AL137493	DKFZP434B1231	*Homo sapiens* mRNA; cDNA DKFZp434B1231 (from clone DKFZp434B1231); partial cds	0.2074
NM007361	NID2	Nidogen 2	0.1986
NM003022	SH3BGRL	SH3 domain binding glutamic acid-rich protein like	0.1773
NM003645	SLC27A2	Fatty-acid-coenzyme a ligase, very long-chain 1	0.1668
BC011762	PIR121	Cytoplasmic FMRP interacting protein 2	0.1580
NM002354	TACSTD1	Tumor-associated calcium signal transducer 1	0.1109
NM024829	FLJ22662	Hypothetical protein FLJ22662	0.1102
AB033073	KIAA1247	Similar to glucosamine-6-sulfatases	0.0930
NM020373	TEME16B	Chromosome 12 open reading frame 3	0.0857
NM031311	CPVL	Carboxypeptidase, vitellogenic-like	0.0847
NM006169	NNMT	Nicotinamide N-methyltransferase	0.0819
AL050125	LOC283824	*Homo sapiens* mRNA; cDNA DKFZp586F071 (from clone DKFZp586F071)	0.0808
NM000735	CGA	Glycoprotein hormones, α polypeptide	0.0781
NM022368	PJA1	Praja 1	0.0714
NM052966	C1orf24	Chromosome 1 open reading frame 24	0.0549
BC012337	FLJ22761	Hypothetical protein FLJ22761	0.0504
NM002639	SERPINB5	Serine (or cysteine) proteinase inhibitor, clade B (ovalbumin), member 5	0.0306
NM007015	LECT1	Chondromodulin I precursor	0.0093

magnification. The slides were evaluated by two experienced pathologists and a consensus was reached. Positive expression for Bcl-2 or MRP3 was defined as >15% staining intensity of tumor cells. The staining of Bcl-2 was mainly localized in the cytoplasm and the staining of MRP3 was localized in the cytoplasm or membrane. Immunohistochemical staining for the Bcl-2 and MRP3 antigen was performed according to the manufacturer's instructions using the standard streptavidin-peroxidase biotin technique with an SP kit (Zhongshan Co., Beijing, China).

Statistical analysis. The SAS statistical software version 9.1 was used for all calculations and statistical analyses. All results were expressed as means ± SD. Statistical significance between treated and untreated groups and analysis of mRNA expression were determined by a Student's t-test. The Dunnett's test was used for evaluation of the inhibitory activity on tumor growth between treated and untreated groups. To assess immunohistochemical data, ANOVA was performed for comparisons between the two groups, Bonferroni's correction was used to compare the multiple comparisons of rate, and correlations between the levels of Bcl-2 and MRP3 were determined using Pearson's correlation analysis. A two-tailed P-value <0.05 was considered to be statistically significant.

Results

Differential gene expression in Anip973 and Anip973/NVB cells by microarray analysis. Expression profiles established from Anip973 and Anip973/NVB cells were based on mean values from triplicate hybridizations. The complete list of these 21571 gene probes was provided as the complete microarray gene expression. One-hundred and forty-three genes were identified as differentially expressed between Anip973 and Anip973/NVB cells. Of these, 55 genes were up-regulated and 88 genes were down-regulated in Anip973/NVB cells

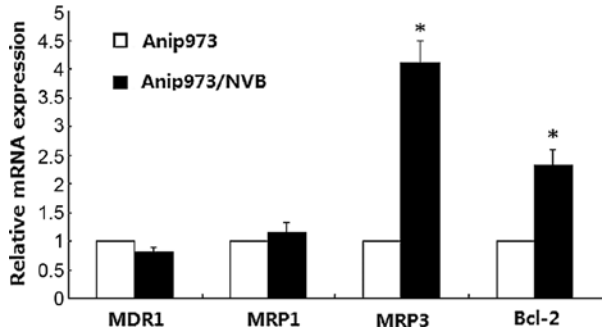

Figure 1. Relative mRNA expression of MDR1, MRP1, MRP3 and Bcl-2 in Anip973 and Anip973/NVB cells. mRNA expression of MDR1 and MRP1 was similar in Anip973/NVB cells relative to those in Anip973 cells. mRNA expression of MRP3 and Bcl-2 was up-regulated in Anip973/NVB cells relative to those in Anip973 cells (*P<0.05).

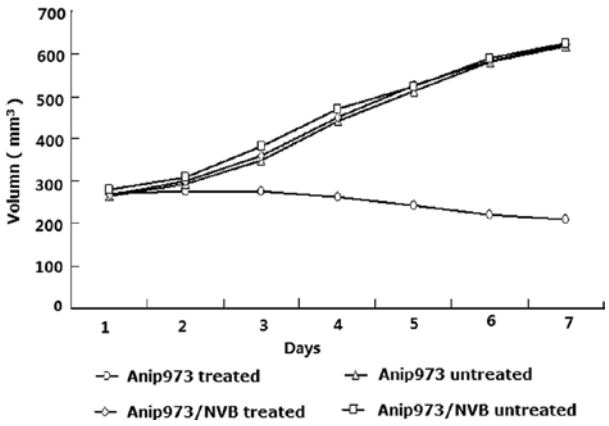

Figure 2. Tumor growth curves of Anip973 cell and Anip973/NVB cell xenografts. After treated by vinorelbine, Anip973 xenografts grew slowly and vinorelbine inhibited the growth of Anip973 xenografts (P<0.001). However, growth of Anip973/NVB xenografts treated by vinorelbine was similar with the 2 untreated groups.

compared to Anip973 cells (Table I). The functions of 143 differently expression genes covered the following: transport, transcription, regulation, signaling, response to stress, metabolism, development, cell organization and biogenesis, cell motility, differentiation, cell cycle, cell adhesion and apoptosis.

qRT-PCR validation of selected genes related to drug-resistance. Four genes known to be related to drug-resistance in cancer cells were selected for validation of the microarray data by qRT-PCR: MDR1, MRP1, MRP3 and Bcl-2 (Fig. 1). Results of qRT-PCR showed that the mRNA levels of MDR1 and MRP1 were similar in the two cell lines (P>0.05). On the other hand, the mRNA levels of MRP3 were higher in Anip973/NVB cells compared with Anip973 cells (P<0.05), which confirmed the microarray data. The mRNA level of Bcl-2 was higher in the Anip973/NVB cells compared with Anip973 cells (P<0.05) as determined by qRT-PCR, although there was no difference in Bcl-2 expression by microarray analysis.

Vinorelbine inhibits xenografts of Anip973 growth but does not affect xenografts of Anip973/NVB growth. Tumor growth curves are shown in Fig. 2. Two days after treatment, tumor growth in the Anip973-treated group became slow, and it was

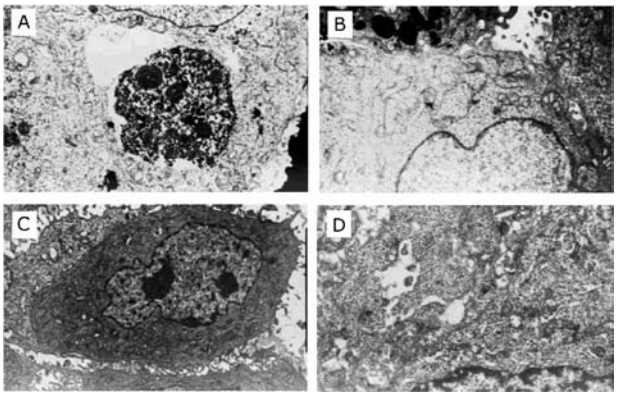

Figure 3. Morphological changes in apoptosis observed in Anip973 and Anip973/NVB xenografts after treatment with vinorelbine by TEM (x10,000). Anip973 cells (A and B) presented apoptosis characteristics, such as cell shrinkage, loss of microvilli and nucleolus, chromatin condensation and formation of apoptotic bodies. No apoptotic changes were observed in Anip973/NVB cells (C and D).

significantly different from the other groups. Seven days after treatment, tumor growth inhibition was obviously observed in the Anip973-treated group. The tumor growth inhibition rates in the Anip973-treated group and the Anip973/NVB-treated group were 60.00% and 4.65% respectively, significantly different between two treated groups (P<0.001). However, there was no significant difference between the tumor growth in the Anip973-untreated group, the Anip973/NVB-untreated group and the Anip973/NVB-treated group (P=0.358).

Vinorelbine induces apoptosis in Anip973 cells, but not in Anip973/NVB cells. Ultrastructural changes were observed by TEM (Fig. 3). Results showed that cells of the Anip973-treated group underwent serial changes, such as cell shrinkage, loss of microvilli and nucleolus, chromatin condensation and formation of apoptotic bodies, which were characteristic of apoptosis in cells. Cytological observations of the Anip973/NVB treated group showed no apoptotic changes and the presence of microvilli and nucleoli and of a large number of well-developed organelles, including Golgi complexes.

Expression of Bcl-2 and MRP3 in tumor xenografts. Higher expression rates of Bcl-2 and MRP3 were observed in Anip973/NVB xenograft cells compared with Anip973 xenograft cells (P<0.001) (Fig. 4). The expression rate of Bcl-2 in the Anip973-treated group, Anip973-untreated group, Anip973/NVB-treated group and Anip973/NVB-untreated group was 47, 48, 74 and 72%, respectively. Moreover, the positive expression rate of MRP3 in the Anip973-treated group, Anip973-untreated group, Anip973/NVB-treated group and Anip973/NVB-untreated group was 53, 52, 79 and 76%, respectively. No correlation was noted between Bcl-2 and MRP3 (P=0.091).

Discussion

As an important anticancer drug, NVB is widely used as chemotherapeutic agent in the treatment of a variety of malignancies, including NSCLC (9), metastatic breast cancer (10), ovarian cancer (11), Hodgkin's disease (12), small cell lung cancer (13), and esophageal carcinoma (14). However, because

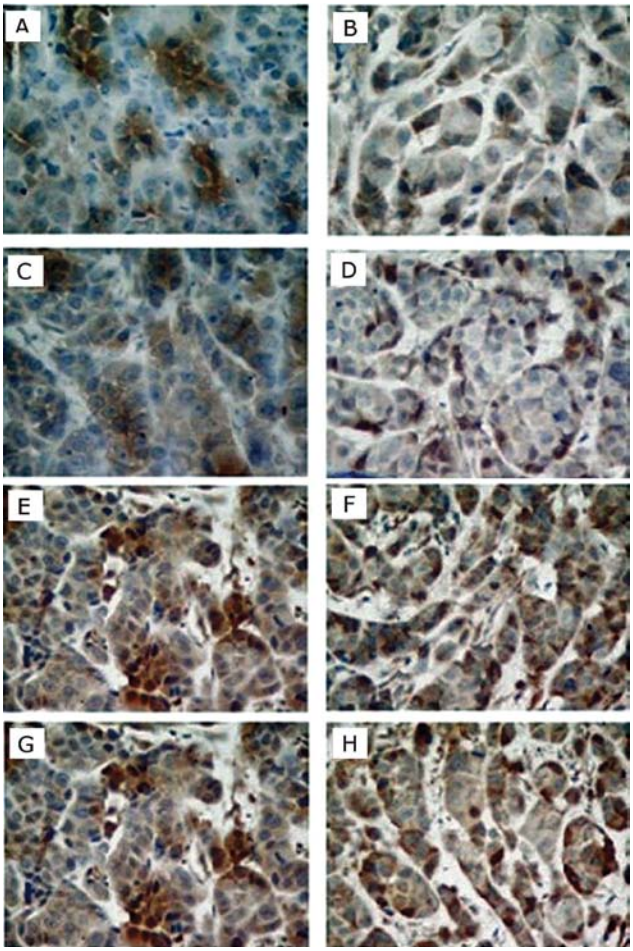

Figure 4. The expression of Bcl-2 (A, C, E and G) and MRP3 (B, D, F and H) in Anip973 and Anip973/NVB xenografts by immunohistochemistry (x400). The expression of Bcl-2 in Anip973/NVB-treated (E) and untreated xenografts (G) was higher than in the Anip973-treated (A) and untreated xenografts (C) and the expression of MRP3 in the Anip973/NVB-treated (F) and untreated xenografts (H) was higher than in the Anip973-treated (B) and untreated xenografts (D) both treated by vinorelbine and saline.

of acquired drug resistance, NVB is not effective after several chemotherapeutic cycles. To study the possible mechanisms of multidrug resistance induced by NVB in lung adenocarcinoma, we established the resistant cell line Anip973/NVB induced by NVB from the parental cell line Anip973, the characteristics of which were confirmed in a previous study (8). Establishment of a multidrug resistance cell line of lung adenocarcinoma was essential and significant for our present study.

In the present study, we first investigated the gene expression variance between the Anip973/NVB and Anip973 cell lines by DNA microarray analysis. This is the first report describing variations in gene expression and genomic alterations of multidrug resistance by NVB in lung adenocarcinomas using microarray technologies. We found that several genes were differentially expressed in the two cell lines, involving cell transport, transcription, regulation, signaling, response to stress, metabolism, development, cell organization and biogenesis, cell motility, differentiation, cell cycle, cell adhesion and apoptosis. Of these genes, the functions of some are still not validated and some genes have multiple functions, therefore selecting genes for further research was difficult. Although some genes were differently expressed significantly between two cells, such as SCAP1, CASP1, ANXA1, AKRIC1, AKRIC4, LECT1, SERPINB5, FLJ22761, C1orf24, PJA1, CGA, LOC283824, NNMT, CPVL, TEME16B, KIAA1247, we decided to study them in the future.

Of the 143 differentially expressed genes, up-regulation of the expression of MRP3 being a drug resistance gene in Anip973/NVB cells was of interest. In addition to MRP3, we selected other classic genes related to drug resistance to confirm the results of our microarray analysis. Results of qRT-PCR showed that the expression of MDR1, MRP1 and MRP3 were in agreement to those of the microarray analysis. However, the mRNA level of Bcl-2 was higher in Anip973/NVB cells compared with Anip973 cells, although no difference was observed in the microarray data between the two cells. We searched the microarray data and found that the ratios of Bcl-2 was 1.7402, 7.5587, 1.7379 respectively in three experiments. As mentioned in our methods, in order to avoid false positive results, only when the ratio of one gene was >2 in all three experiments, the gene was considered to show a significant differential expression between the two cell lines. It is for this reason that Bcl-2 was excluded from the differential genes identified by microarray analysis. Nevertheless, we identified a trend for Bcl-2 up-regulation in Anip973/NVB cells compared with Anip973 cells by both methods.

To examine the response of Anip973 and Anip973/NVB cells to NVB *in vivo*, we established mice xenograft models. We found that Anip973/NVB xenografts resisted NVB therapy, which reconfirmed the characteristics of Anip973/NVB cells. We did not observe cell apoptosis by TEM in Anip973/NVB xenografts after NVB therapy, suggesting that anti-apoptosis may be one of the drug-resistance mechanisms. Furthermore, we performed immunohistochemistry to observe the expression of Bcl-2 and MRP3 protein. As expected, higher expression of Bcl-2 and MRP3 were demostrated in Anip973/NVB xenografts cells compared with Anip973 xenograft cells, that further validated our findings of gene variation.

P-glycoprotein (MDR1) and multidrug resistance protein 1 (MRP1) play an important role in the extrusion of drugs from cancer cells and their overexpression can be a cause of failure of anticancer drugs in numerous cancers (15,16). Results both from DNA microarray analysis and qRT-PCR showed that MDR1 and MRP1 were not responsible for resistance to NVB in the present study.

Belonging to the ATP-binding cassette (ABC) multidrug transporters that constitute the MRP family, MRP3 is an organic anion transporter capable of transporting anticancer agents, and it can actively efflux lipophilic anions and hydrophobic compounds and contribute to multidrug resistance in cancers (17,18). Originally, investigators reported that MRP3 mRNA levels were strongly correlated with resistance to doxorubicin, vincristine, etoposide and cisplatin in lung cancer cells (19,20). Subsequently, MRP3 was found that it contributed to 5-fluorouracil resistance in pancreatic carcinoma cells (21). Huang *et al* (22) found that MRP3 contributed to vincristine resistance in human cancer cells, however, this was cell-selective and was not necessarily dependent on pregnane X receptor-mediated effects. Furthermore, MRP3 also contributed to adriamycin resistance in human hepatocellular

carcinoma cells and tetramethylpyrazine could effectively reverse the multi-drug resistance (23). The results of our study showed that mRNA and protein expression of MRP3 were higher in Anip973/NVB cells than in Anip973 cells, indicating that MRP3 may participate in NVB resistance in lung adenocarcinoma. According to NVB being a lipophilic and hydrophobic drug, we speculated that MRP3 may efflux NVB from cells and contribute to multidrug resistance in lung adenocarcinoma.

Although proteins that interfere with either drug accumulation or efflux contribute to drug resistance, other factors also play an important role. One major mechanism of drug resistance in cancer cells is the defective apoptosis pathway (24,25). In our study, we also found that up-regulation of Bcl-2 may be involved in multi-drug resistance induced by NVB in lung adenocarcinoma. It is known that Bcl-2 is an important anti-apoptotic protein that can regulate cancer cell apoptosis and prolong cell survival (26). In addition, Bcl-2 has been known to confer resistance to chemotherapeutic agents in a variety of human cancers (27). Studies in acute myeloid leukemia (AML) have revealed that high levels of Bcl-2 were associated with resistance to chemotherapy and antisense oligodeoxynucleotides targeting Bcl-2 mRNA could increase sensitivity of AML cells to arabinocytosine *in vitro* (28,29). Researchers found that overexpression of Bcl-2 was associated with resistance to chemotherapy-induced apoptosis in pancreatic cancer and the ERK/Bcl-2 pathway may confer resistance of pancreatic cancer to anoikis (30,31). As reported, we consider that Bcl-2 confers drug resistance by preventing NVB-induced cell death in lung adenocarcinoma in the present study, that was confirmed by results observed through TEM.

In summary, we identified a set of genes that were responsible for multidrug resistance induced by NVB in lung adenocarcinoma. Among them, contribution of MRP3 and Bcl-2 were confirmed *in vitro* and *in vivo*. However, a great number of factors are documented to be associated with drug resistance in human cancer. In future studies we plan to investigate other differentially expressed genes identified using DNA microarray and further study the mechanism of NVB drug resistance in lung adenocarcinoma.

Acknowledgements

We thank Dr Sun Xilin for excellent advice on preparing the manuscript. This study was supported by the Scientific and Technological Innovative Project of Harbin (no. 2006RFXXS037).

References

1. Marty M, Extra JM, Espie M, *et al*: Advances in vinca-alkaloids: Navelbine. Nouv Rev Fr Hematol 31: 77-84, 1989.
2. Rahmani-Jourdheuil D, Coloma F, Placidi M, *et al*: Human hepatic uptake of two vinca alkaloids: navelbine and vincristine. J Pharm Sci 83: 468-471, 1994.
3. Vokes EE, Rosenberg RK, Jahanzeb M, *et al*: Multicenter phase II study of weekly oral vinorelbine for stage IV non-small-cell lung cancer. J Clin Oncol 13: 637-644, 1995.
4. Gebbia V, Caruso M, Valenza R, *et al*: Vinorelbine plus cisplatinum for the treatment of stage IIIB and IV non small cell lung carcinoma. Anticancer Res 14: 1247-1249, 1994.
5. Green MR: New directions for chemotherapy in non-small-cell lung cancer. Chest 103 (Suppl 4): S370-S372, 1993.
6. Muller M, Meijer C, Zaman GJ, *et al*: Overexpression of the gene encoding the multidrug resistance-associated protein results in increased ATP-dependent glutathione S-conjugate transport. Proc Natl Acad Sci USA 91: 13033-13037, 1994.
7. Hipfner DR, Deeley RG and Cole SP: Structural, mechanistic and clinical aspects of MRP1. Biochim Biophys Acta 1461: 359-376, 1999.
8. Chen GY, Yang ZY, Hong X, *et al*: Establishment of a multi drug-resistant human lung adenocarcinoma cell line and biological characteristics. Zhonghua Yi Xue Za Zhi 87: 924-926, 2007.
9. Rinaldi M, Cauchi C and Gridelli C: First line chemotherapy in advanced or metastatic NSCLC. Ann Oncol 17: 64-67, 2006.
10. Domenech GH and Vogel CL: A review of vinorelbine in the treatment of breast cancer. Clin Breast Cancer 2: 113-128, 2001.
11. Harries M and Kaye SB: Recent advances in the treatment of epithelial ovarian cancer. Expert Opin Investig Drugs 10: 1715-1724, 2001.
12. Devizzi L, Santoro A, Bonfante V, *et al*: Vinorelbine: a new promising drug in Hodgkin's disease. Leuk Lymphoma 22: 409-414, 1996.
13. Weinmann M, Jeremic B, Bamberg M, *et al*: Treatment of lung cancer in elderly part II: small cell lung cancer. Lung Cancer 40: 1-16, 2003.
14. Bidoli P, Aglione S, Toffolatti L, *et al*: New strategies in the treatment of esophageal cancer. Minerva Chir 57: 717-731, 2002.
15. He SM, Li R, Kanwar JR, *et al*: Structural and functional properties of human multidrug resistance protein 1 (MRP1/ABCC1). Curr Med Chem 18: 439-481, 2011.
16. Li X, Li JP, Yuan HY, *et al*: Recent advances in P-glycoprotein-mediated multidrug resistance reversal mechanisms. Methods Find Exp Clin Pharmacol 29: 607-617, 2007.
17. Borst P and Elferink RO: Mammalian ABC transporters in health and disease. Annu Rev Biochem 71: 537-592, 2002.
18. Kruh GD and Belinsky MG: The MRP family of drug efflux pumps. Oncogene 22: 7537-7552, 2003.
19. Young LC, Campling BG, Voskoglou-Nomikos T, *et al*: Expression of multidrug resistance protein-related genes in lung cancer: correlation with drug response. Clin Cancer Res 5: 673-680, 1999.
20. Oguri T, Isobe T, Fujitaka K, *et al*: Association between expression of the MRP3 gene and exposure to platinum drugs in lung cancer. Int J Cancer 93: 584-589, 2001.
21. Hagmann W, Jesnowski R, Faissner R, *et al*: ATP-binding cassette C transporters in human pancreatic carcinoma cell lines. Up-regulation in 5-fluorouracil-resistant cells. Pancreatology 9: 136-144, 2009.
22. Huang R, Murry DJ, Kolwankar D, *et al*: Vincristine transcriptional regulation of efflux drug transporters in carcinoma cell lines. Biochem Pharmacol 71: 1695-1704, 2006.
23. Wang XB, Wang SS, Zhang QF, *et al*: Inhibition of tetramethylpyrazine on P-gp, MRP2, MRP3 and MRP5 in multidrug resistant human hepatocellular carcinoma cells. Oncol Rep 23: 211-215, 2010.
24. Johnstone RW, Ruefli AA and Lowe SW: Apoptosis: a link between cancer genetics and chemotherapy. Cell 108: 153-164, 2002.
25. Reed JC: Dysregulation of apoptosis in cancer. J Clin Oncol 17: 2941-2953, 1999.
26. Zhou F, Yang Y and Xing D: Bcl-2 and Bcl-xL play important roles in the crosstalk between autophagy and apoptosis. FEBS J 278: 403-413, 2011.
27. Reed JC: Bcl-2-family proteins and hematologic malignancies: history and future prospects. Blood 111: 3322-3330, 2008.
28. Tóthová E, Fricova M, Stecová N, *et al*: High expression of Bcl-2 protein in acute myeloid leukemia cells is associated with poor response to chemotherapy. Neoplasma 49: 141-144, 2002.
29. Campos L, Sabido O, Rouault JP, *et al*: Effects of BCL-2 antisense oligodeoxynucleotides on in vitro proliferation and survival of normal marrow progenitors and leukemic cells. Blood 84: 595-600, 1994.
30. Bold RJ, Chandra J and McConkey DJ: Gemcitabine-induced programmed cell death (apoptosis) of human pancreatic carcinoma is determined by Bcl-2 content. Ann Surg Oncol 6: 279-285, 1999.
31. Galante JM, Mortenson MM, Bowles TL, *et al*: ERK/BCL-2 pathway in the resistance of pancreatic cancer to anoikis. J Surg Res 152: 18-25, 2009.